Hindawi
Advances in Civil Engineering
Volume 2021, Article ID 5590448, 8 pages
https://doi.org/10.1155/2021/5590448

Research Article

Effect of Superficial Scratch Damage on Tension Properties of Carbon/Epoxy Plain Weave Laminates

Miaomiao Duan,[1,2] **Zhufeng Yue**,[1] **and Qianguang Song**[3,4]

[1]*School of Mechanics, Civil Engineering and Architecture, Northwestern Polytechnical University, Xi'an 710129, China*
[2]*School of Urban Planning and Municipal Engineering, Xi'an Polytechnic University, Xi'an 710048, China*
[3]*Beijing Institute of Structure and Environment Engineering, Beijing 100076, China*
[4]*Tianjin Aerospace Reliability Technology Co., Ltd., Tianjin 300462, China*

Correspondence should be addressed to Miaomiao Duan; mmduan@xpu.edu.cn

Received 5 February 2021; Revised 12 March 2021; Accepted 20 March 2021; Published 1 April 2021

Academic Editor: Guang-Liang Feng

The effect of scratch damage on the tension properties of carbon fiber plain weave laminates has been studied in detail using digital image correlation (DIC) and acoustic emission (AE). A range of scratch lengths was machined onto different laminates. The bearing capacity of the laminates was then compared with that of unaltered samples. The strain field distributions near the scratches were measured and analyzed as a function of scratch length with DIC. Initiation and propagation of damage were monitored during the tensile tests using AE. Failure sites and morphologies were observed and analyzed. The results show that superficial scratches have little effect on the strength of plain weave laminates when the scratch length is less than 80% of the specimen width. Scratches affect the distribution of strain near the scratch but not far away from the scratch or at the back face of the sample. Not all samples broke from the scratch site but instead broke from the free edge of the sample or close to the gripping region.

1. Introduction

Composite materials are increasingly used for many important applications in industry, especially in aerospace. This is due to their significantly higher strength, stiffness, and versatile design. Despite these desirable properties, composite structures are susceptible to defects during both manufacturing and in service. This includes the creation of phenomena such as holes, notches, delamination, and scratches. These defects will inevitably affect the structural integrity and structural load-bearing capability of the materials [1–4]. Several studies of damage to composites have focused on the response and performance of composite structures that have been subjected to low- or high-velocity impact [5–8].

Superficial cracks and/or scratches in composite materials may occur, for example, from concrete or other runway debris during aircraft takeoffs and landings. Scratches can also occur via routine ground maintenance operations such as winter deicing operations or mechanical accidents such as tool-drops or abrasion from a sharp object. Scratches can cut into the fibers of some of the plies, which can in turn induce high interlaminar stress and stress concentration. This type of damage can eventually degrade static strength and fatigue strength of the composite structure, making the laminates with scratches more vulnerable to failure under an external load.

Plain weave laminates composed of interlocking fibers and a polymer matrix generally exhibit superior overall performance and are less sensitive to damage than traditional laminated composite materials. For this reason, a deeper understanding of the effects of scratch damage on plain weave laminates is important for the designing of safer structural materials for the aerospace industry, especially when considering the range of possible service conditions. Recently, several research groups have reported studies

regarding the scratch-resistant behavior of composite materials from a tribology perspective, i.e., determining best practices for reducing the wear potential and for protecting the subsurface condition [9–12].

There are significantly fewer studies published regarding the effects of scratches on the mechanical properties of weave laminates. There is a report of the effect of scratches reaching different depths on the delamination of a laminated composite under tensile loading, using experimental and numerical analysis techniques [13]. The results indicated that the scratch tip location and depth are dominant factors for tension load capacity and that scratches can result in undesirable bending and torsional deformations, leading to additional delamination. The influence of different stacking sequences on the failure mode of composite laminates with scratches under tensile loading has also been investigated [14]. Bora et al. studied the effect of scratch resistance on fiber orientation for polymer composites and presented the scratch resistance of polyetherimide composites as a function of scratch hardness, penetration depth, and the coefficient of friction [15]. Size effects in quasi-isotropic carbon/epoxy laminates with the through-thickness center-notches have also been reported [16]. In particular, they used 3-D CT to examine damage ahead of the crack tips and then compared their samples with those of open-hole laminates using the same material, the same stacking sequence, and the same overall dimensions. The discrete ply modeling method has been used to conduct a computational study on notched tensile tests, which analyzed the influence of dimensions, notch shape, and the stacking sequence [17].

All of these previous studies focused on the effect of deep scratches or gouges on the mechanical properties of composite laminates. Here, we present a detailed analysis of the tensile properties of carbon fiber plain weave laminates exposed to more superficial scratches. Our goal is to characterize the effect of different scratch lengths on the mechanical properties of plain weave laminates. The mechanical properties under investigation in this work are tensile strength, distribution of strain, and identification of failure modes.

2. Materials and Methods

2.1. Materials. The material used in these experiments was a composite consisting of a thermoset epoxy resin reinforced with carbon fiber braids (T700GCSC-12K-50C, Toray Industries, characteristics are listed in Table 1). E_1 and E_2 are the elasticity moduli in the fiber direction and the transverse direction, respectively, and G_{12} and G_{23} are the shear moduli in-plane and out of the plane, respectively. The term ϑ_{12} is Poisson's ratio.

Six layers of bidirectional plain weave carbon fabric $[0/90]_6$ were stacked together. The samples (length = 250 mm and width = 25 mm) were cut from plain weave plates using a waterjet cutting machine. The geometry and dimensions of the specimens used for this study are illustrated in Figure 1. Different scratch lengths (5, 10, 15, 20, and 25 mm) were machined using a CNC (computer numerical control) milling machine at the center of the sample. The scratch depth for all specimens was 0.4 mm which is approximately 15% of the test sample thickness. This depth is relatively shallow compared with most of studies on scratches so is called superficial scratch in this paper. The 25 mm scratch length was evident throughout the width of the specimen. To ensure reproducibility of the results, five specimens were tested under the same conditions.

Table 1: Properties of T700SC-12K-50C

E_1/GPa	E_2/GPa	ϑ_{12}	G_{12}/MPa	G_{23}/MPa
55.8	54.9	0.0538	4200	3700

Note. E_1 and E_2 are the elasticity moduli in the fiber direction and in the transverse direction, respectively, and G_{12} and G_{23} are the shear moduli in-plane and out of plane, respectively, and the term ϑ_{12} is Poisson's ratio.

2.2. Methods. DIC is a full-field optical technique that measures displacements on the surface of an object that has been subjected to mechanical, thermal, or various environmental loadings. For these samples, the strain is evaluated via differentiation of the displacement fields. The DIC technique has been widely proven as an advanced and direct technique for measuring full-field strain or displacement [18–20]. In this work, DIC was used to capture surface displacements and evaluate strain in scratched laminate specimens under tensile load.

The AE signals were recorded by using two AE sensors with an optimum frequency range of 100–750 kHz. A 40 dB preamplifier was used to monitor damage progression. The AE sensors were mounted at both ends of the gauge section on the back face of the sample. This positioning allows for DIC monitoring on the scratched face. Before each test, the pencil lead break method was used several times to calibrate the AE sensors according to the ASTM E976-10 standard. The contact surface of the sensor was covered with silicon grease to create good acoustical coupling between the AE sensors and the sample face.

Tensile tests on plain weave laminates were conducted according to ASTM Standard D3039 [21] as shown in Figure 2(a). An Instron 8801 fatigue testing system with a load cell capacity of 100 kN was used to apply a constant displacement to the sample at a speed of 2 mm/min. The tensile load during the test was measured using the load cell. DIC measurements were used to determine the full-field strains at different points in the loading regime, by tracking random speckle patterns on the scratched specimens. Three strain gauges were mounted at points A, B, and C (Figure 2(c)) on the scratched back face and two AE sensors were mounted on the back face of the sample to monitor damage initiation and propagation.

3. Results and Discussion

3.1. Tensile Strength. Representative force-displacement curves of the scratched samples are shown in Figure 3. The curves show an almost linear response up to the point of final failure. Small load drops were observed in some tests at 70–80% of the final failure load, but they are not obvious.

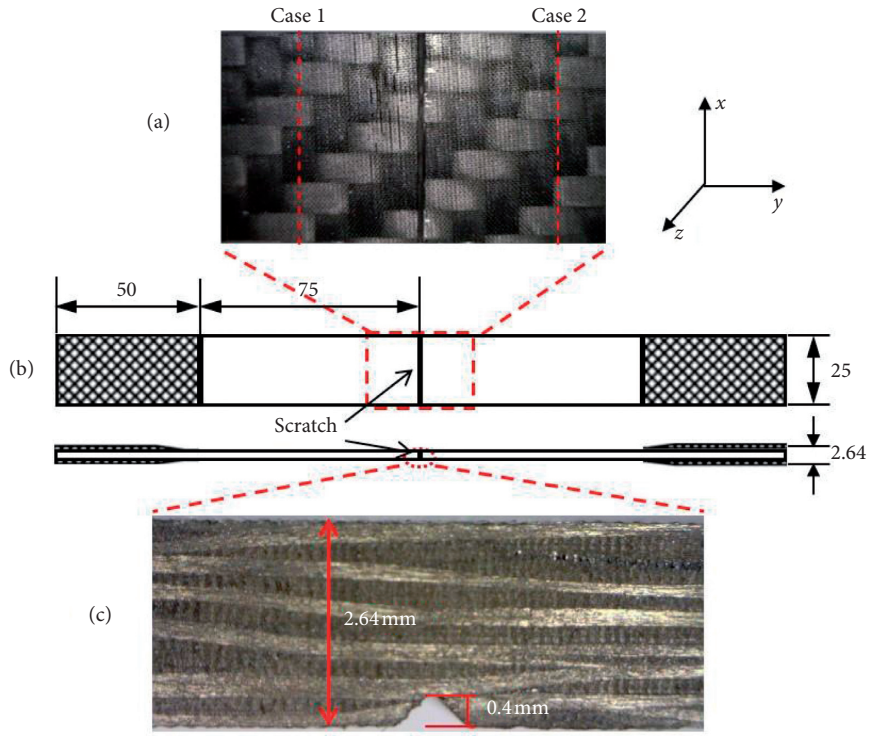

Figure 1: Geometry and dimensions of a representative sample with a 25 mm scratch length.

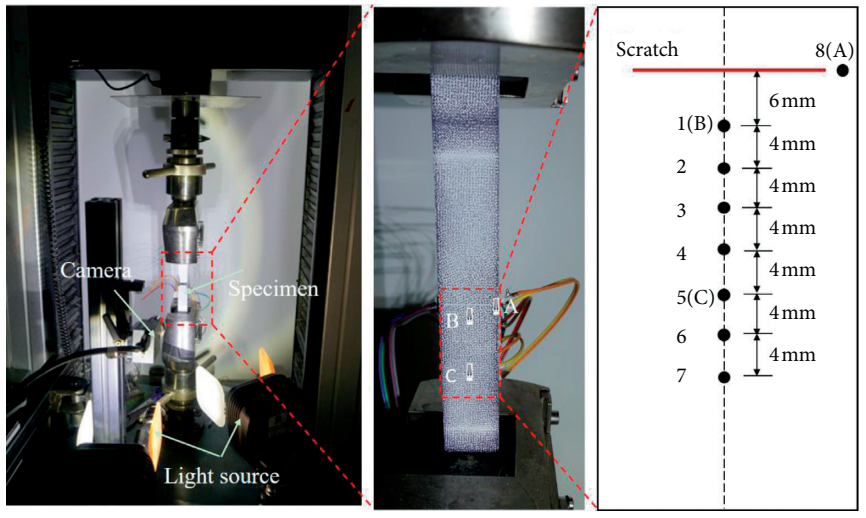

Figure 2: (a) Experimental setup for tensile tests. (b) Photo of the scratched sample. Points A, B, and C denote the locations of the strain gauges on the back face of the sample. (c) Points 1–8 denote the locations of strain evaluated using DIC.

This phenomenon indicates that some fiber breakage occurred in the sample, but they still maintained a bearing capacity. The final failure of all samples was catastrophic and the loads dropped immediately. The failure loads of all specimens are shown in Table 2 and compared with an undamaged sample. In Table 2, W is the width of the sample and CV refers to the coefficient of variation. From Table 2, it could be noted that samples with 5 mm, 10 mm, and 15 mm scratch lengths had an insignificant effect on failure loads. However, longer scratch lengths (20 mm and 25 mm) degraded the tensile strength by 5.4% and 9.75%, respectively, compared with the undamaged sample. This meant that the scratch length could be too small to affect the bearing capacity of the structure. However, if the scratch length was longer than 80% of the specimen width, the scratched materials, in particular the first layer of the sample, resulted in a significant reduction in the bearing capacity of the structure. From Table 2, it was also noted that under the

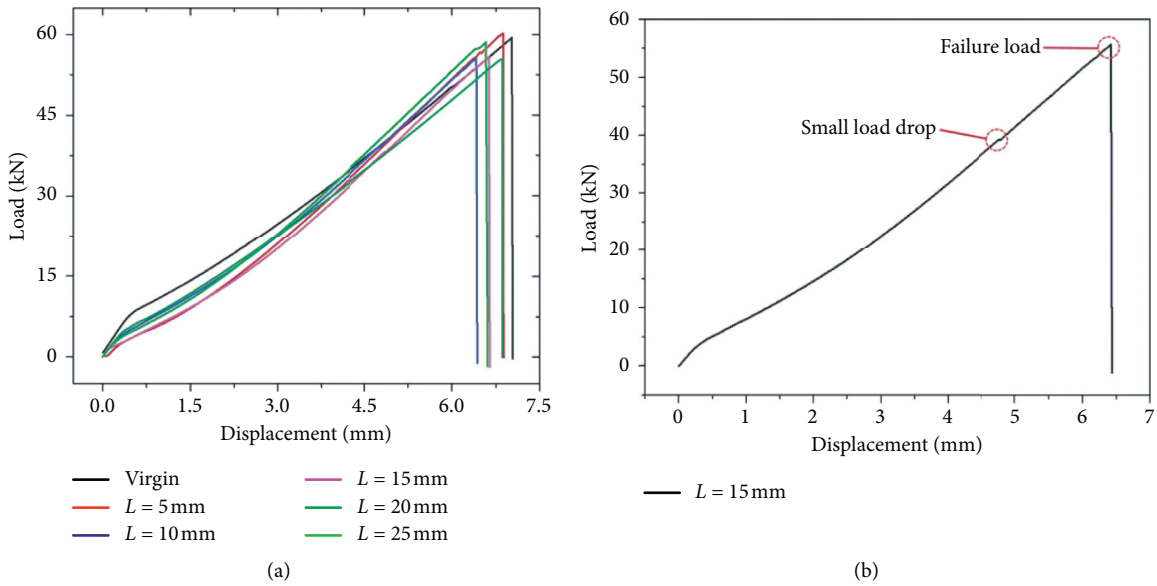

Figure 3: Load-displacement curves.

Table 2: Bearing capacity loads compared between different scratch lengths and virgin specimen.

Specimen	Average failure load (kN)	CV (%)	Load reduction (%)
Virgin	59.28	10.88	—
$L = 5$ mm (20% W)	57.66	10.23	2.83
$L = 10$ mm (40% W)	58.48	4.93	1.35
$L = 15$ mm (60% W)	59.17	6.60	0.19
$L = 20$ mm (80% W)	56.08	3.82	5.40
$L = 25$ mm (100% W)	53.50	10.70	9.75

same conditions, the variation coefficient of the failure load was relatively large. There were two reasons for this observation. Firstly, one of the characteristics of these composite materials was their larger dispersion. Secondly, the scratch position (Figure 1(a)) of plain weave laminates might play a significant role in controlling the bearing capacity of the sample. For case 1, the scratch cuts more warp yarn, which could result in a lower bearing capacity. However, for case 2, the scratch was laid in the intersection between the warp and weft yarns, which effectively cuts less warp yarn and therefore had less influence on the bearing capacity.

3.2. Normal Strain Distribution. Figures 4–6 show DIC results in terms of engineering strain plots ε_{yy} (loading direction) at the location points 1–8 that are previously indicated in Figure 2(c). The same trend in strain distribution of samples with 5 mm, 10 mm, and 15 mm and 20 mm scratch lengths was observed; therefore, further discussion has been made using the results on samples with 15 mm and 25 mm scratch lengths. From Figure 4(a), it was noted that high axial strain concentration occurred at the scratch tip (point 8), especially at the later loading stage. In Figure 4, longitudinal strain at different points shows different trends during the tensile process. At the initial loading stage, the strain at all points increased linearly until the load was increased to 25 kN, followed by a drop at point 1. The closer the point was to the scratch, the earlier the strain decreased, while at points farther away from the scratch, the strain always increased as the load was increased. This phenomenon could be explained as follows: as only part of the fiber in the first layer was cut off, when the load was relatively small, the strain was uniform in distribution. As the load was increased, the scratch was pulled apart and the scratch width became larger. As a free boundary, the material at the scratch showed large interlaminar stress, which resulted in delamination between the first and second layers, causing the strain in the vicinity of the scratch to decrease. With increasing load, the delamination process gradually extended from the scratch to both ends of the sample, and the strain at other points was correspondingly decreased. Surface scratches make the strain near the scratch decrease with the increase in load at the later loading stage, and the strain at the scratch tip increases rapidly with the increase in load due to the existence of the high strain concentration phenomenon. It could be concluded that scratch only affects the distribution of strain near the scratch but does not affect strain far away from the scratch. The affected range was

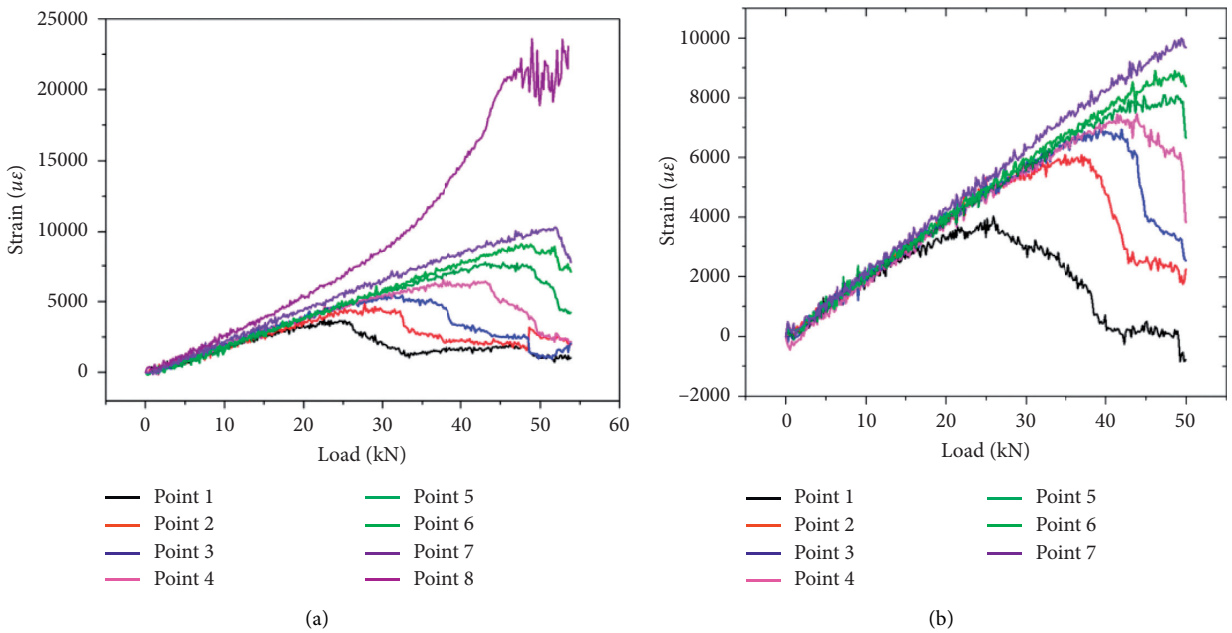

Figure 4: Strain-load curves of specimen with (a) $L = 15$ mm and (b) $L = 25$ mm.

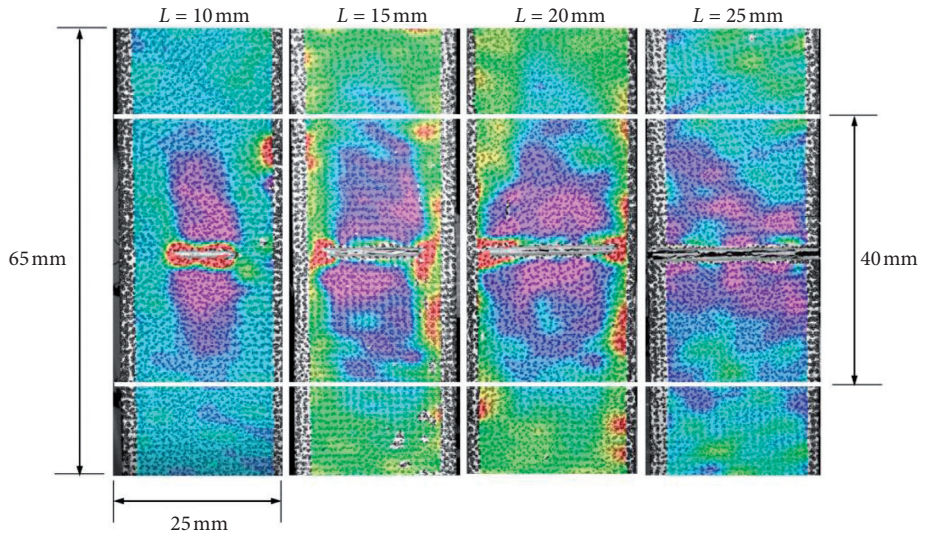

Figure 5: The strain fields under failure load.

about 40 mm (Figure 5) which is 16% of the test sample length. Figure 5 shows that different scratch lengths had an insignificant effect on the affected range of strain in the plain weave laminates.

The strain fields ε_{yy} obtained using the DIC technique at different applied tensile load levels are shown in Figure 6. The results showed high localized strain closer to scratch. Strain concentration occurred around the scratch for samples with a scratch length through the width (25 mm), but the strain concentration of other samples occurred at both ends of the scratch. Figure 6 also highlights the fact that with increased load, the affected range of the scratch on strain distribution was increased gradually.

A comparison of strain values between the gauges on the back face of the samples ($L = 15$ mm) with the DIC results on the scratch face is shown in Figure 7. The position of points 1, 5, and 8 should show results similar to the strain gauges (Figure 2(c)). Figure 7 shows that the strain stayed almost the same for the initial loading stage until the load reached 25 kN except point 8. After this load value, points 1 and 8 in the vicinity of the scratch could be distinguished from the other points due to damage. The strain of point 8 is higher than that of other points after 8 kN, especially at the later loading stage. Because point 8 is located at the tip of the scratch, there is a large strain concentration phenomenon which becomes more and more obvious with the increase in load. The conclusion could be drawn that the scratch only affected

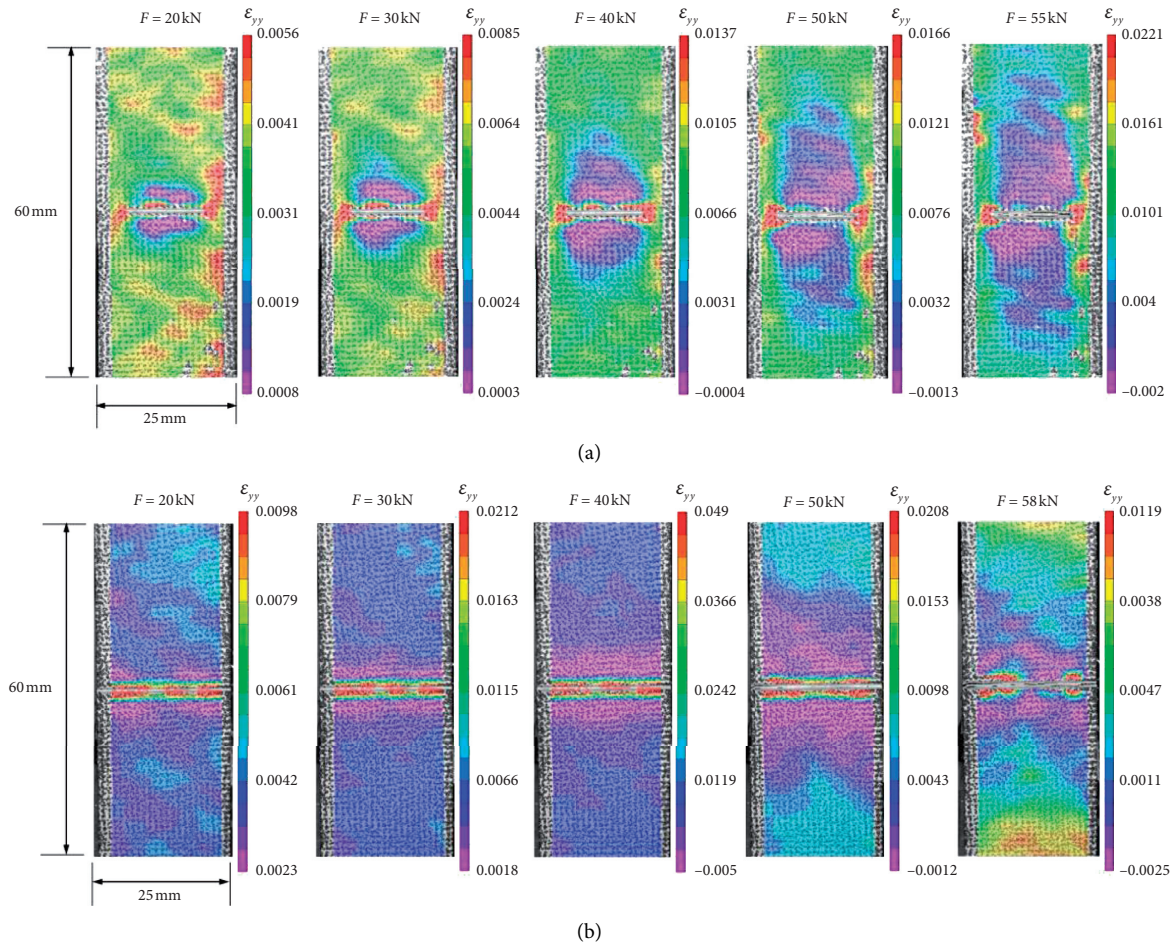

Figure 6: Strain fields ε_{yy} obtained using the DIC technique during testing: (a) $L = 15$ mm and (b) $L = 25$ mm.

the distribution of the strain near the scratch (about 40 mm) but did not affect the strain far away from the scratch (point 5) and at the back face (points A, B, and C).

3.3. Failure Mechanisms. Figure 8 shows the load-time and AE cumulative energy-time curves for the $L = 25$ mm sample. According to Figure 8, the AE cumulative energy curve could be divided into three regions. In region I, at the initial damage stage (0–170 s), the corresponding load was 0–25 kN. At the beginning of the loading, the AE signal was generated. The cumulative energy was relatively low, and it barely increased with an increase in the load. There was slight damage to the sample, but the damage expanded slowly. Due to the high preparation temperature of the composite material and the mismatch between the thermal expansion coefficient of the fiber and the matrix, thermal stress was generated when the sample was cooled to room temperature after preparation, resulting in microcracks in the matrix. AE signals at this stage were mainly generated when microcracks expanded in the matrix and the interface.

In region II, interfacial damage between the fiber and the matrix (170–235 s) was observed, and the corresponding load was 25–34 kN. The AE cumulative energy increased gradually as the load was increased, which indicated that the macrocracks in the matrix expanded steadily and delamination was initiated at the scratch, accompanied by some fiber breakage. However, the sample still had a load-bearing capacity, which was as per the DIC results. In region III, i.e., the fiber breakage stage (235–340 s), the corresponding load was 34–48 kN. The AE cumulative energy increased rapidly and reached a maximum, which indicated that more fibers started to break until the sample was completely failed.

From the experimental results, it was found that not all samples broke from the scratch site. Failure sites were classified as follows: (a) scratch location, (b) gauge length (except for scratch location), and (c) grip section, as illustrated in Figure 9. Figure 10 helps to explain the reasoning for the failure sites. In Figure 10, the black boxes denote the locations of strain concentration. From Figure 10, it could be noted that when the sample has broken, strain concentration might occur at the scratch site, the free edge of the sample, and close to the gripping region, corresponding to all three failure sites. Localized strain concentration determined the failure onset of the entire sample.

Figure 11 shows failure morphology of scratch specimen. The fracture was disorganized, and a large amount of fiber breakage and delamination was observed. A large number of

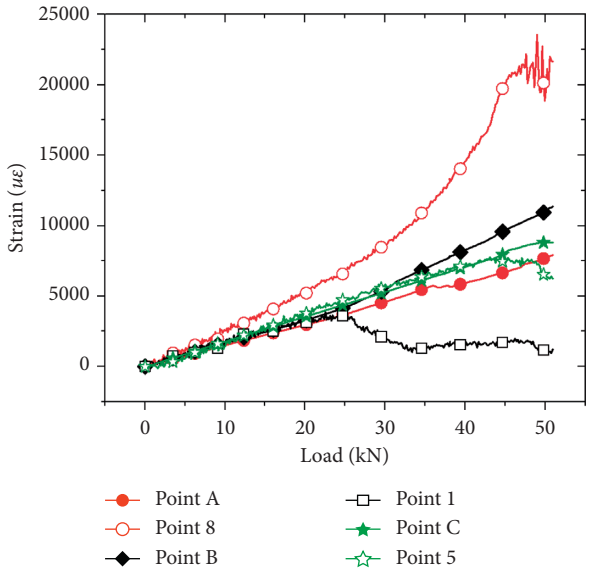

Figure 7: Comparison of strain values between gauge measurements and DIC results.

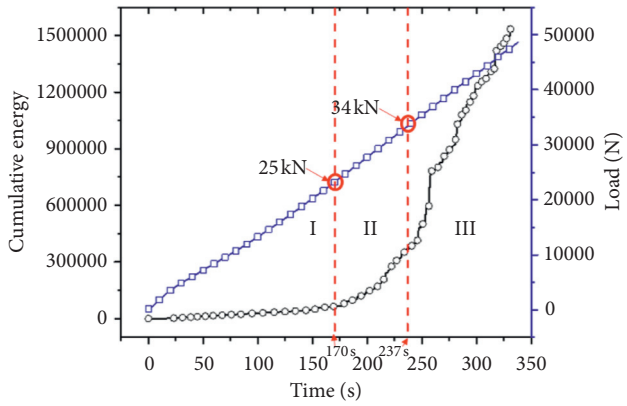

Figure 8: Load-time and AE cumulative energy-time curves for specimen ($L = 25$ mm).

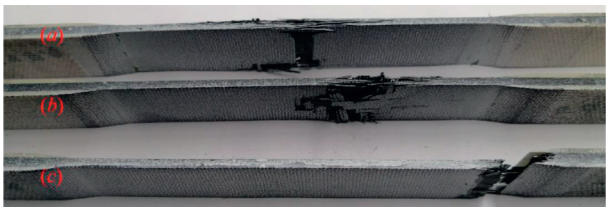

Figure 9: Failure sites of scratched samples.

fiber bundles were detached from the plain weave laminate, and the resin fell off the surface. This was because the tensile strength of the fiber bundles was greater than the binding power between the fibers and the resin; therefore, the fibers and the resin were separated from the plain weave laminate. The scratch rendered the first weave layer unrestrained in the loading direction, resulting in a lowered bearing capacity.

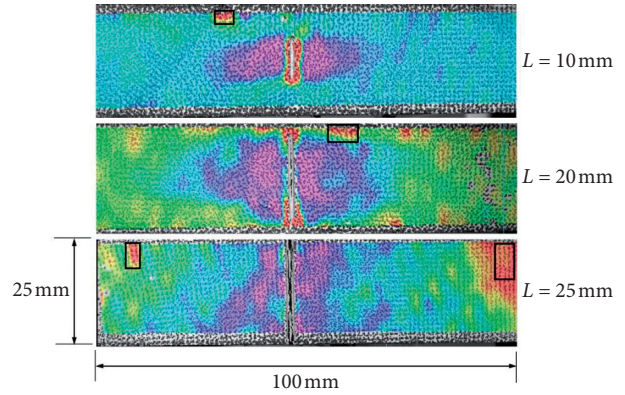

Figure 10: Strain fields ε_{yy} of scratched samples under failure load.

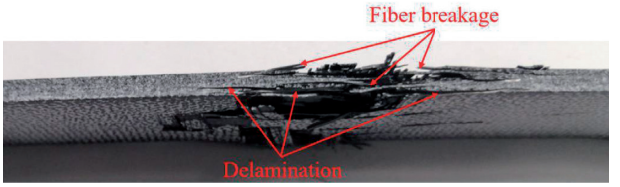

Figure 11: Fracture morphology of a representative scratched sample.

This made the fiber prone to separation, tearing, and rapid failure. When the fiber in the first weave layer failed, the crack expanded rapidly along the fiber direction, eventually causing delamination.

4. Conclusions

In this study, the experimental tensile load investigations of carbon/epoxy plain weave laminates with different scratch lengths were presented and discussed. The normal strain distribution around the scratches was measured, and the fracture site and morphology were observed. Several conclusions could be drawn from these experiments:

(1) The effect of superficial scratches was insignificant in terms of tensile strength when the scratch length was small. Relatively lower tensile strengths were observed in the samples when the scratch length was more than 80% of the sample width. This was attributed to the first layer of the samples having almost no bearing capacity.

(2) Superficial scratches make the strain near the scratch decrease with the increase in load at the later loading stage, and the strain at the scratch tip increases rapidly with the increase in load. Scratching was also found to only affect strain distribution near scratch, with an effective range being 16% of the test sample length. The strain far away from scratch and at the back face was unaffected. Different scratch lengths had no significant effect on the affected range of strain in plain weave laminates.

(3) The failure mechanisms of plain weave laminates with superficial scratches were characterized by fiber breakage, leading to delamination. The failure site of some samples was not at the scratch site because localized strain concentration might have occurred at the scratch site, the free edge of the sample, or close to the gripping region.

Data Availability

The data used to support the findings of this study are included within the article.

Conflicts of Interest

The authors declare no potential conflicts of interest with respect to the research, authorship, and/or publication of this article.

Acknowledgments

This work was supported by the Natural Science Foundation of Shaanxi Province (No. 2017JM5018).

References

[1] J. Awerbuch and M. S. Madhukar, "Notched strength of composite laminates: predictions and experiments," *Journal of Reinforced Plastics and Composites*, vol. 4, pp. 153–159, 1985.

[2] F. K. Chang and K. Y. Chang, "A progressive damage model for laminated composites containing stress concentrations," *Journal of Composite Materials*, vol. 2, no. 21, pp. 834–855, 1987.

[3] R. F. El-Hajjar and D. R. Petersen, "Gaussian function characterization of unnotched tension behavior in a carbon/epoxy composite containing localized fiber waviness," *Composite Structures*, vol. 93, no. 9, pp. 2400–2408, 2011.

[4] C. Soutis and J. Lee, "Scaling effects in notched carbon fibre/epoxy composites loaded in compression," *Journal of Materials Science*, vol. 43, no. 20, pp. 6593–6598, 2008.

[5] S. Long, X. Yao, and X. Zhang, "Delamination prediction in composite laminates under low-velocity impact," *Composite Structures*, vol. 132, pp. 290–298, 2015.

[6] H. R. Wang, S. C. Long, X. Q. Zhang, and X. H. Yao, "Study on the delamination behavior of thick composite laminates under low-energy impact," *Composite Structures*, vol. 184, pp. 461–473, 2018.

[7] H. Tuo, Z. Lu, X. Ma, C. Zhang, and S. Chen, "An experimental and numerical investigation on low-velocity impact damage and compression-after-impact behavior of composite laminates," *Composites Part B: Engineering*, vol. 167, pp. 329–341, 2019.

[8] C. T. Key and C. S. Alexander, "Numerical and experimental evaluations of a glass-epoxy composite material under high velocity oblique impacts," *International Journal of Impact Engineering*, vol. 137, pp. 1–10, 2020.

[9] V. Bharathi, M. Ramachandra, and S. Srinivas, "Influence of fly ash content in aluminium matrix composite produced by stir-squeeze casting on the scratching abrasion resistance, hardness and density levels," *Materials Today: Proceedings*, vol. 4, no. 8, pp. 7397–7405, 2017.

[10] R. D. K. Misra, R. Hadal, and S. J. Duncan, "Surface damage behavior during scratch deformation of mineral reinforced polymer composites," *Acta Materialia*, vol. 52, no. 14, pp. 4363–4376, 2004.

[11] Y. N. Liang, S. Z. Li, R. H. Zhang, and S. Li, "Effect of fiber orientation on a graphite fiber composite in single pendulum scratching," *Wear*, vol. 198, no. 1-2, pp. 122–128, 1996.

[12] Z. Zhang, I. A. Alhafez, and H. M. Urbassek, "Scratching an Al/Si interface: molecular dynamics study of a composite material," *Tribology Letters*, vol. 66, pp. 85–96, 2018.

[13] S. Seyedmohammad and F. E. Rani, "Effects of scratch damage on progressive failure of laminated carbon fiber/epoxy composites," *International Journal of Mechanical Sciences*, vol. 67, pp. 70–77, 2013.

[14] R. P. Derek, F. E. Rani, and A. K. Bashar, "On the tension strength of carbon/epoxy composites in the presence of deep scratches," *Engineering Fracture Mechanics*, vol. 90, pp. 30–40, 2012.

[15] M. O. Bora, O. Çoban, T. Sinmazcelik, and V. Gunay, "Effect of fiber orientation on scratch resistance in unidirectional carbon-fiber-reinforced polymer matrix composites," *Journal of Reinforced Plastics and Composites*, vol. 29, no. 10, pp. 1476–1490, 2010.

[16] X. Xu, M. R. Wisnom, Y. Mahadik, and S. R. Hallett, "An experimental investigation into size effects in quasi-isotropic carbon/epoxy laminates with sharp and blunt notches," *Composites Science and Technology*, vol. 100, pp. 220–227, 2014.

[17] J. Serra, C. Bouvet, B. Castanié, and C. Petiot, "Experimental and numerical analysis of carbon fiber reinforced polymer notched coupons under tensile loading," *Composite Structures*, vol. 181, pp. 145–157, 2017.

[18] J. Cuadra, P. A. Vanniamparambil, K. Hazeli, I. Bartoli, and A. Kontsos, "Damage quantification in polymer composites using a hybrid NDT approach," *Composites Science and Technology*, vol. 83, pp. 11–21, 2013.

[19] M. A. Caminero, S. Pavlopoulou, M. Lopez-Pedrosa, B. G. Nicolaisson, C. Pinna, and C. Soutis, "Analysis of adhesively bonded repairs in composites: damage detection and prognosis," *Composite Structures*, vol. 95, pp. 500–517, 2013.

[20] J. J. Andrew, V. Arumugam, D. J. Bull, and H. N. Dhakal, "Residual strength and damage characterization of repaired glass/epoxy composite laminates using A.E. and D.I.C." *Composite Structures*, vol. 152, pp. 124–139, 2016.

[21] ASTM D3039, *Standard Test Method for Tensile Properties of Polymer Matrix Composite Materials*, ASTM International, West Conshohocken, PA, USA, 2007.